PHYSICAL REVIEW A VOLUME 14, NUMBER 6 DECEMBER 1976

Charge dependence of K x-ray production in nearly symmetric collisions of highly ionized S and Cl ions in gases*

J. R. Macdonald, M. D. Brown,† S. J. Czuchlewski,‡ and L. M. Winters§
Kansas State University, Manhattan, Kansas 66506

R. Laubert,‖ I. A. Sellin, and J. R. Mowat¶
University of Tennessee, Knoxville, Tennessee 37916
and Oak Ridge National Laboratory, Oak Ridge, Tennessee 37830

(Received 26 July 1976)

Using gas targets, K x-ray cross sections have been measured as a function of projectile charge state in nearly symmetric collisions for highly ionized S and Cl ions at a velocity comparable to that of the K-shell electrons. For bare nuclei, the projectile cross sections are accurately described by the cross section for capture to excited states calculated in a Brinkman-Kramers approximation and normalized by a single scaling factor. With lower-charge-state incident ions, the total K-vacancy cross section is in good agreement with the $2p\pi$-$2p\sigma$ cross section for rotational coupling.

I. INTRODUCTION

It is well established that the cross section for production of x rays in energetic ion-atom collisions shows a strong monotonic increase with the charge state of the incident projectile,[1] and mechanisms responsible for the phenomenon have been discussed qualitatively. For example, multiple vacancies produced in inner (as well as outer) shells have been shown to depend on projectile configuration, giving rise to significant changes in the mean fluorescence yield of ion-excited atoms.[2] In other cases, variations in atomic structure cannot fully account for the charge-state dependence, but variations in inner-shell vacancy production must also occur.[3] If the mechanism for ionization in a fast collision is predominantly direct Coulomb ionization, one can include variations in nuclear screening or electron binding energy in an explanation of the projectile charge dependence of vacancy production.[4] Estimates of the contribution of electron capture processes[5] have shown that this mechanism can account for the charge dependent trends of vacancy production. For relatively slow collisions, the promotion of inner-shell electrons by the coupling of molecular states[6] has been used to describe successfully the dependence of vacancy production on projectile charge state.

In experimental work that has been reported to date, the measurements of projectile charge dependence have pertained either to asymmetric projectile-target combinations at high energy [>1 MeV/amu][1] or to nearly symmetric collisions at lower energy [<100 keV/amu].[6] In this paper, measurements of the charge dependence of x-ray production cross sections are reported for approximately symmetric collision systems at high energy. It is obvious that the projectile K x radiation from incident bare nuclei results from electron capture to excited states. For these incident ions, the contribution of electron capture of target K electrons is expected to make a significant contribution, as well, to the target K-vacancy production cross section.[7] The charge dependence of the target x-ray cross sections measured in this work are discussed within this framework. For lower-charge-state incident ions, the measured cross sections of both projectile and target K x rays are examined in terms of K-vacancy sharing and theoretical cross sections for electron promotion by rotational coupling of molecular states.[8]

II. EXPERIMENTAL METHODS

For this experiment chlorine and sulphur beams of the same velocity (3.77 MeV/amu), and a chlorine beam of lower velocity (3.0 MeV/amu) from the MP tandem Van de Graaff accelerator at Brookhaven National Lab (BNL) were employed. Following stripping of each momentum-analyzed beam in a thin carbon foil, single incident charge states were magnetically selected and focused through a thin gas target. The double-differentially-pumped gas cell apparatus that was transported under vacuum from KSU to BNL has been described in detail previously.[9] The target gases used were Ne, SiH_4, H_2S, HCl, and Ar. Target and projectile K x rays were counted in a Si(Li) x-ray detector which was mounted within the gas cell so that its field of view did not encompass the target apertures. The detector resolution was 190 eV at 5.9 keV, and 174 eV at 2.3 keV. The energy response was calibrated both with standard sources and by proton bombardment of the target gases. Below the peak of an x-ray line, the spectral dis-

tribution consisted of a decreasing tail that contained 16 ± 2% of the line intensity for x rays in the range from 1.7 to 3.0 keV. It was necessary to consider this contribution in obtaining the relative intensities when the target x rays are dominated by projectile x rays at slightly higher energy in the nearly symmetric collisions of this experiment.

The low-energy spectral tail results from incomplete charge collection in the edges of the detector, and to account for this tail in extracting relative intensities of the several lines in each of the heavy-ion spectra, a one-parameter function consisting of a Gaussian peak of variable width and a linear representation of the tail was used to describe each line analytically. The choice of this simple response function to provide an adequate correction for the tail was made by investigating the simple spectra produced by proton bombardment of the target gases. Of course, multiparameter fitting functions provided better, but not unique, analytic fits over the entire spectral range, but the straight-line tail, decreasing from 8% of the peak maximum to zero at the detector noise level, accurately followed the tail out to four peak widths, and was chosen to include the entire intensity contribution from the tail. After subtraction of background spectra, taken with no gas, the total number of counts in the tail was reproduced to an accuracy of 2% of the total peak intensity by the analytic fit.

With each of the target gases, x-ray spectra were taken at two pressures (approximately 10 and 20 mTorr) with 3.77-MeV/amu chlorine and sulphur ions incident as bare nuclei, one-, two-, and three-electron ions. Additional spectra were taken with lower-charge-state S ions and with 3.0-MeV/amu Cl ions in all available charge states in SiH_4. The spectra obtained for the various collision systems differ markedly, and several examples are shown in Fig. 1. Background spectra were obtained with only residual gas (<0.1 mTorr) in the cell for each incident ion, and this small contribution was subtracted from each spectrum prior to analysis. For all charge states of S and Cl ions incident on Ne and SiH_4 gases, and in some cases with the other gases, the detector resolution was sufficient to use peak-fitting programs[10] to extract peak centroid energies, widths, and relative intensities from each spectrum independently.

Initial fitting of the data at BNL was attempted using a Gaussian fitting routine and treating the low-energy tail as a background. For well-separated peaks, such as seen in the upper two spectra of Fig. 1 (for Cl^{+17} and Cl^{+14} on SiH_4), this was satisfactory as long as the relative intensities were normalized to the total number of x rays in

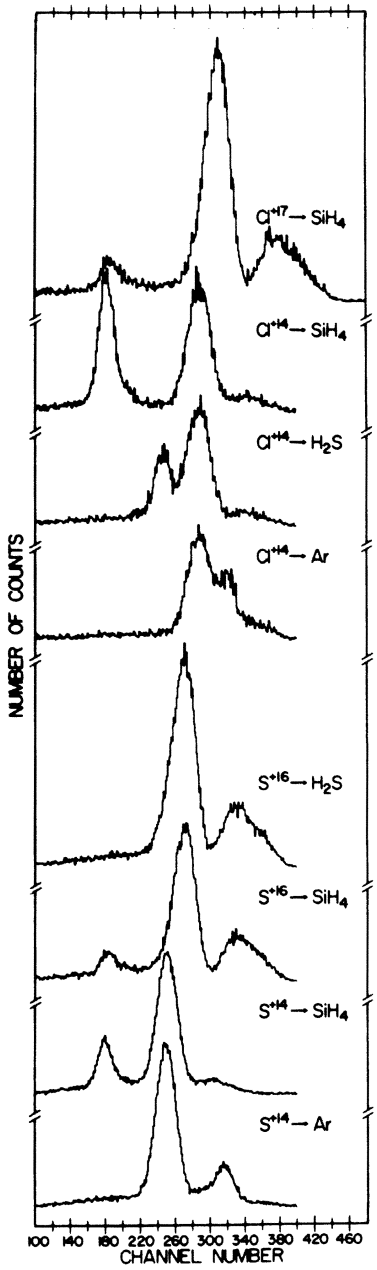

FIG. 1. Typical spectra.

the spectrum. For close peaks, even if well resolved, as in the sixth spectrum in Fig. 1 (for Cl^{+14} on H_2S), this was unsatisfactory, giving even relative errors in excess of 25%. Hence, the data were reanalyzed at KSU using a program containing the proper spectral response for each peak. The program converged on three peaks in the spectrum as long as either of the following conditions was met. The smaller peaks were resolved down to half maximum, as seen in Fig. 1 in the third (for S^{+16} on SiH_4) and the sixth spectra

(for Cl^{+14} on H_2S). Or, poorly resolved peaks were in order of decreasing intensity with increasing channel number, as seen in Fig. 1, for the highest peak in the second spectrum (for S^{+14} on SiH_4) and for all the peaks in the fifth spectrum (for Cl^{+14} on Ar). For other cases, portions of the spectra did not converge in the fitting program to give separate peaks. For example the program was not adequate to resolve the small low-energy shoulder arising from target x rays, from the main peak seen in the fourth spectrum of Fig. 4 (for S^{+16} on H_2S). Nor could two peaks be fit to the upper portion of the first spectrum in Fig. 1 (for S^{+14} on Ar). For these and similar cases, some assumptions were required to retrieve all the information from the spectra.

In all cases where the spectra were resolvable, the distribution of projectile x rays was found to be independent of target gas for each projectile charge state. To retrieve relative intensity information from partially resolved features in the spectra obtained with H_2S, HCl, and Ar target gases, this target independence was applied as a general constraint in the analysis. With this assumption, the projectile x-ray distribution and the background distribution for each incident charge state are obtained over the entire spectral range of the detector by forming a composite from the well-resolved portions of the spectra taken with different targets. These distributions were used in a spectral-stripping procedure[11] to extract systematically the relative intensity and distribution of target K x rays produced in the nearly symmetric collisions. In all cases, the distribution obtained with this procedure was a single group of target K x rays.

The possibility of error in the relative intensity of x rays extracted by the peak-stripping technique varies greatly from one collision system to another, and this is reflected in the difference in the uncertainty of the individual cross sections presented in Sec. III. The centroid energy for the target x-ray group could be determined in some cases, but with greater uncertainty than for the projectile groups. For Cl in HCl, and S in H_2S, the separation into projectile and target components was possible only because of the presence of a significant resolved $K\beta$ component from projectiles but not for target atoms. The dominance of the projectile radiation over that from the target permitted an accurate determination of the former, but resulted in an uncertainty of 30–40% in the latter.

Cross sections for x-ray production were determined by normalizing the relative intensities obtained in the spectral analysis to the total number of x rays. Absorption in the 0.025-cm Be window separating the detector from the gas cell introduces a detection efficiency[12] that varies from 0.56 for 1.74-keV Si K x rays to 0.86 for 2.96-keV Ar K x rays. Values of efficiency, accurate to a few percent, were chosen corresponding to the centroid energy for the Si, S, Cl, and Ar K x-ray groups identified in this experiment. A large relative, as well as absolute, uncertainty in the approximately 2.5% efficiency for Ne K x rays, precludes the determination of accurate Ne K x-ray cross sections for this target.

A capacitance manometer was used to monitor the gas target pressure and provided normalization of the target density with a relative precision of 1% and with an absolute uncertainty of 10%. Beam current normalization was achieved by integrating the total charge collected in a large, suppressed, Faraday cup in the high-vacuum region behind the target. Complete transmission through the cell was ensured by geometrical considerations and was confirmed by the measurement of current collected in a removable Faraday cup inside the cell and on the insulated exit apertures of the apparatus.

In the conversion of current normalization to particle normalization, estimates of the effect of charge exchange[13] in the cell were included. In all cases, less than 10% of the beam undergoes charge exchange in the target. For most charge states, beam current in excess of 0.2 nA could be obtained through the gas cell. The total uncertainty in particle normalization was less than 5% in these cases. For the highest charge states less beam was obtained, and a surface barrier detector replaced the Faraday cup for beam normalization. With this technique the useable beam was limited by the particle counting rate so that statistical uncertainties limited the accuracy of x-ray yields obtained in a reasonable amount of time. In some cases, yields were measured with both methods of normalization and the results agreed within 8%, comparable to the statistical uncertainty obtained with normalization by single particle counting.

The apparatus geometrical factor required to obtain absolute cross sections from the normalized yields was determined by measuring the yield of Ar K x rays produced by 3.77-MeV protons. This yield was normalized to the cross section of $8.0 \pm 0.6 \times 10^{-22}$ cm^2 measured for this radiation in a separate experiment.[14] The absolute uncertainty in the measured cross sections is limited to 8% by this normalization, but it makes the results independent of the absolute calibration of the beam integrator, and pressure normalization. The relative uncertainty in the cross sections is determined by the spectral analysis, detector efficiency, dead-time corrections, corrections for beam transmission through the target, charge exchange

in the target, and statistics in some cases. The total uncertainty in the cross sections reported in the next section was obtained by adding the absolute and relative uncertainties in quadrature.

III. RESULTS AND DISCUSSION

A. General trends of x-ray cross sections

In this experiment, the K x rays emitted by the projectiles form the dominant spectral features when the incident ions carry K-shell vacancies into the collision. For lower charge states the total cross sections are reduced by more than an order of magnitude and K radiation from the target is of comparable intensity to that from the projectile. This overall charge-state dependence is evident in Fig. 2, in which the K x-ray cross sections for Cl incident on SiH_4 at 3.0 and 3.77 MeV/amu are shown for ions carrying n electrons into the collisions. For clarity in the figure, data points for the same incident state are displaced when projectile and target cross sections overlap. The trends of these cross sections are typical of all those measured in this experiment; hence a general discussion of the results will be given before all the results are presented in detail.

The Cl K x-ray cross sections for $n=0$ and 1, shown in Fig. 2, are almost a factor of 2 larger for the lower-energy than the higher-energy collisions, while the Si K cross sections are about 10% larger.

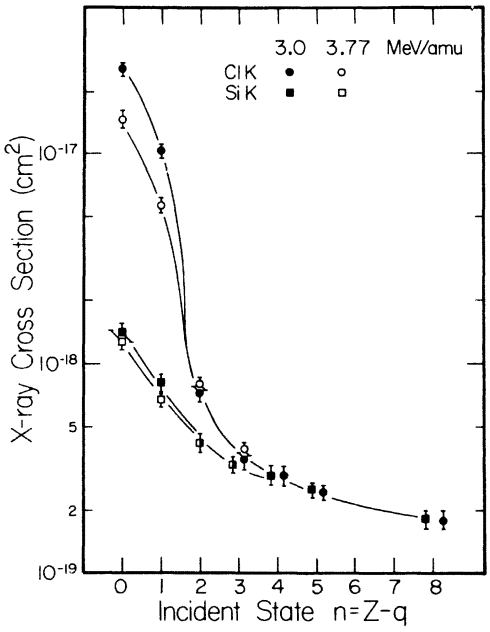

FIG. 2. Target and projectile K x-ray production cross sections as a function of the number of electrons on the incident projectile.

Such a decrease with energy is characteristic of the general trend of high-velocity electron-capture cross sections. For example, the energy dependence of the capture cross section to excited states calculated in a Brinkman-Kramers calculation[15] for Cl nuclei incident on Si is shown in Fig. 3 by the solid line. Projectile x-ray cross sections from this experiment are also shown in the figure. The calculated cross section has been reduced by an order-of-magnitude for normalization purposes, but reproduces the general trend of the experimental data.

It is expected that capture is the mechanism for x-ray production for projectiles carrying K vacancies into the collision. However, the observation that the energy dependence for the target cross section is in the same direction to that of the projectile cross section is evidence for a contribution of K-shell capture to the target vacancy production.

When a second electron is present on the incident ion, the projectile cross section is reduced by approximately an order-of-magnitude, but is still a factor of 2 larger than the cross section with three-electron ions. Since it is reasonable to expect a substantial component of $^3S_1$ metastable ions in these incident two-electron beams, with this ion, the observed x rays result from a combination of $^3S_1$ to $^3P_1$ excitation in the collisions, as well as inner-shell excitation, or ionization concurrent with outer-shell electron capture. These effects will be discussed further in Sec. III B.

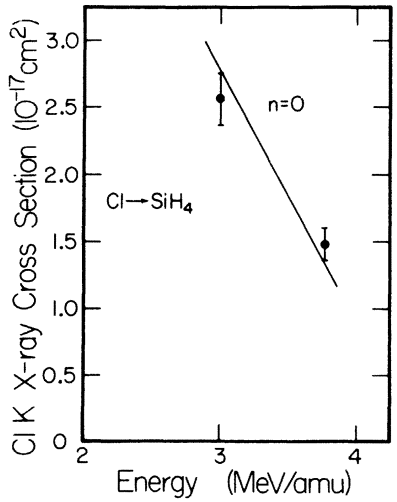

FIG. 3. Projectile x-ray cross section for bare nuclei of Cl incident on SiH_4 at 3.77 MeV/amu. The solid line shows the energy dependence of the cross section for capture to excited states calculated in a Brinkman-Kramers approximation and reduced by an order of magnitude.

For the ions entering the collision with full K shells, $n>2$, the cross sections shown in Fig. 2 are comparable for the target and projectile, and show no energy dependence. The collision velocities of the experiment match the mean velocity of the K-shell electrons, and hence we anticipate that the observed cross sections are near the peak of the excitation function. These cross sections also show a gradual decrease with increasing n. This may reflect a decrease in final-state fluorescence yield or a reduction in the K-vacancy production cross section with the addition of L-shell electrons to the projectile.

Results obtained with the other target gases and with sulphur ions show a charge dependence similar to those shown for $Cl \rightarrow SiH_4$ in Fig. 2. In Sec. III B the quantitative results will be discussed for the projectile radiation, and in Sec. III C for the target radiation.

B. Projectile K x-ray energies and cross sections

With the detector resolution of 180 eV, the K x rays emitted by the projectiles are separated into two resolvable groups. Even for the thin gas targets used, the lower energy $K\alpha$ group represents several satellite lines making the observed FWHM of this peak range from 260 to 300 eV. The FWHM of the higher energy group ranged from 460 to 520 eV, and the designation $K\beta$ is nominal; transitions from higher shells make contributions to the peak also.

Centroid energies for the $K\alpha$ and $K\beta$ projectile groups were obtained with a precision of 9 and 27 eV, respectively, from the analysis of the spectra. For a specific incident charge-state ion, the centroid energy (and the width) of the $K\alpha$ and $K\beta$ groups, as well as the $K\beta$-to-$K\alpha$ intensity ratio, were independent of the target within the precision of the measurements. These parameters were also the same for the two different energy chlorine ions. Values of $K\alpha$ and $K\beta$ centroid energies, averaged for all targets obtained for incident ions carrying n electrons are shown in Fig. 4. For comparison, allowed $2p \rightarrow 1s$ transitions[16] for one-, two-, and three-electron sulphur and chlorine ions are shown in the figure as the horizontal lines beside the data points representing the observed $K\alpha$ energies. Similarly, estimates of $3p \rightarrow 1s$ transitions,[17] with various numbers of electrons on the ions, are shown in the figure.

With incident bare nuclei, $n=0$, projectile x rays signal the decay of the excited states formed by electron capture. The $K\alpha$ energies, shown in Fig. 4, for this incident state correspond to Lyman-α transitions in hydrogen-like ions, and the $K\beta$ centroids are comparable to the Lyman-β energy.

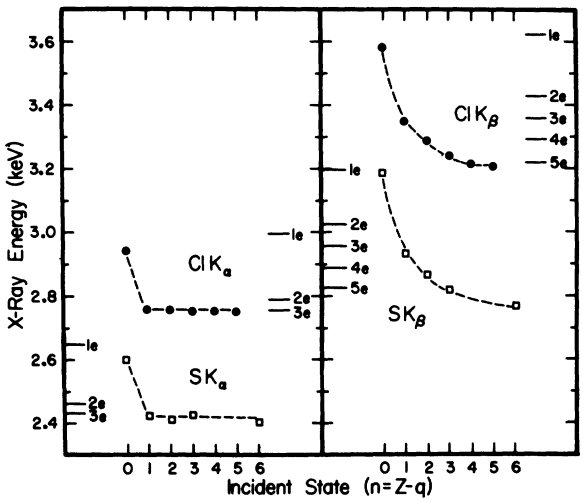

FIG. 4. Projectile K x-ray energies observed in this experiment as a function of the number of electrons on the incident projectile. The horizontal lines are theoretical x-ray energies determined for the lowest configuration containing an initial K vacancy and the indicated number of electrons.

For the other incident states, the $K\alpha$ centroid is independent of the charge state, at an energy corresponding to $2p \rightarrow 1s$ transitions in helium-like or lithium-like ions. In contrast, there is a monotonic decrease in centroid energy of the $K\beta$ group with additional electrons present on the incident projectile. A similar monotonic decrease is observed in the charge dependence of the $K\beta$-to-$K\alpha$ intensity ratio shown in Fig. 5. These features are the same with both S and Cl ions incident on all of the targets.

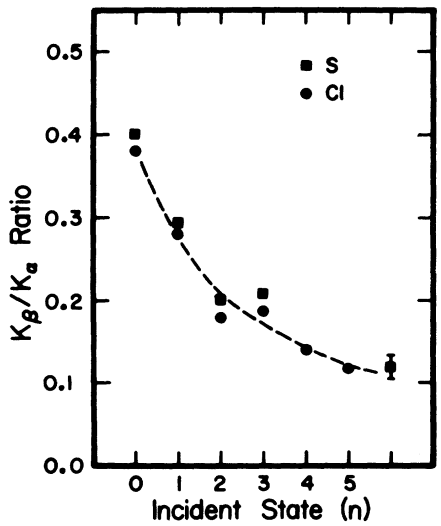

FIG. 5. $K\beta$-to-$K\alpha$ intensity ratio for the projectile radiation observed as a function of the number of electrons on the incident ions.

The observation of the $K\beta$ radiation for all incident charge states, initially without M electrons, is indicative of the importance of electron capture to excited states of these highly ionized projectiles. This conclusion is confirmed by the results of calculations, in the Brinkman-Kramers (BK) approximation,[15] which show that the dominant capture processes are to projectile excited states. As an illustration of the trend of these calculations, cross sections for capture to projectile states with a given principal quantum number from a particular target shell are shown in Fig. 6 for the case of 3.77-MeV/amu chlorine in collision with argon. Results obtained for other projectile-target combinations differ in detail, but have the same general trends to those shown in the figure.

Although these calculated results pertain to projectiles with $n=0$, the presence of inner-shell electrons on the incident ion will screen the nuclear charge and reduce the cross section for capture to excited states, as calculated in a BK approximation. For the collision systems of this experiment, the reduction is small and there is a large probability of capture to outer shells in collisions which produce K vacancies in the lower-charge incident ions ($n \geq 2$). Radiative decay of these captured electrons to the ground state is in competition with

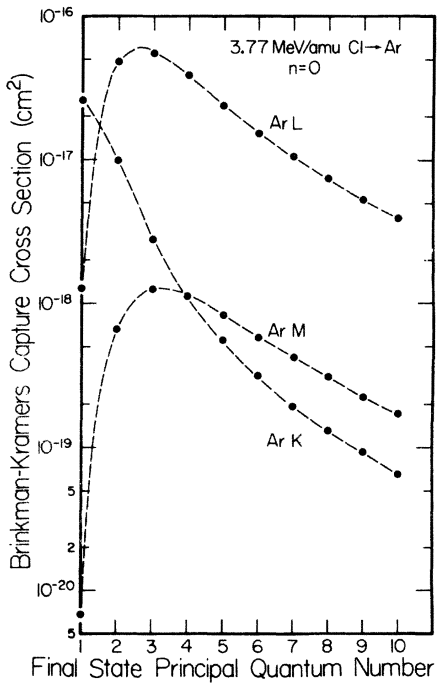

FIG. 6. Cross sections for electron capture by bare nuclei of Cl from particular shells of Ar to all final states with a particular principal quantum number. The calculations are made in a Brinkman-Kramers approximation.

the filling of K vacancies by the L-shell electrons present on the projectile. The mode of decay of the projectile K-shell vacancies depends sensitively on the L- and higher-shell populations, and the sharp reduction in $K\beta/K\alpha$ ratio with increasing n may reflect an increase in K-LL and K-LM Auger decay at the expense of K-M radiative decay. The constancy of the $K\alpha$ energy for the lower-charge-state incident ions shows that the stripping of L-shell electrons in these collisions also plays a role, and that normally only one or two L-shell electrons are present during the radiative process.

Total cross sections for the production of K x rays from the highly ionized Cl and S projectiles of this experiment are listed in Table I. The measured values represent the cross section for collisions with the heavy atoms in the target molecules, since the presence of the hydrogen atoms makes a negligible contribution to the total projectile cross section. For example, for low-charge-state S and Cl ions, the x-ray cross section caused by collisions with hydrogen at 3.77 MeV/amu will be comparable to the K x-ray cross section for S and Cl excited by 3.77-MeV protons. These cross sections were measured to be 980 and 940 b, respectively, in conjunction with this experiment. This amounts to a contribution of less than 0.5% of the total projectile cross section. In addition, for incident bare nuclei, the electron capture cross section to excited states of Cl or S from hydrogen is calculated to be only 10^{-3} of that from Ne, Si, S, Cl, or Ar atoms.[15] Hence with all charge states we can consider the hydrogen atoms as spectators to the interaction with the heavier atoms in the target.

The trends of cross sections for incident projectiles carrying n electrons are shown in Fig. 7 as a function of the target atomic number. For incident bare nuclei, $n=0$, the largest x-ray cross sections observed in this experiment are a measure of the cross section for electron capture to excited states, reduced by a factor $f \leq 1$, to account for the fraction of the transitions that do not yield K x rays but lead to $2s$ final states by either direct capture or cascading. In principle, the factor f can be determined if a complete distribution of angular momentum states populated by electron capture is calculated and then known branching ratios are used to calculate f. In the absence of a theoretical formulation other than the Brinkman-Kramers approximation for calculating these cross sections, such detail is not warranted. In fact, it is well known that a Brinkman-Kramers calculation reproduces the relative trends of cross sections, but grossly overestimates the magnitude of electron-capture cross sections by a factor g, that may be a function of velocity and be different for

TABLE I. Projectile K x-ray cross sections (10^{-19} cm^2).

Target / Incident state $n = Z - q$	Chlorine ions						Sulphur ions				
	105 MeV		132 MeV				120.7 MeV				
	SiH_4	Ne	SiH_4	H_2S	HCl	Ar	Ne	SiH_4	H_2S	HCl	
0	257 ± 20	95 ± 8	148 ± 13	165 ± 17	199 ± 22	232 ± 25	72 ± 6	105 ± 9	153 ± 16	155 ± 17	178 ± 18
1	103 ± 9	54 ± 4	57 ± 4	79 ± 8	82 ± 9	98 ± 11	31 ± 2	41 ± 3	53 ± 6	60 ± 7	69 ± 7
2	7.2 ± 0.7	7.0 ± 0.5	8.0 ± 0.5	8.8 ± 1.0	8.0 ± 1.6	8.6 ± 1.0	6.7 ± 0.5	9.8 ± 0.7	10.1 ± 1.4	11.1 ± 1.3	11.3 ± 1.2
3	3.4 ± 0.3	3.1 ± 0.2	3.9 ± 0.3	5.0 ± 0.6	4.4 ± 0.6	4.8 ± 0.6	3.7 ± 0.2	4.8 ± 0.3	4.9 ± 0.7	5.6 ± 0.7	5.6 ± 0.6
4	2.9 ± 0.3						...	...	...	...	...
5	2.4 ± 0.2						...	...	...	...	...
6	...						2.2 ± 0.2	2.9 ± 0.2	3.1 ± 0.4	3.3 ± 0.4	3.6 ± 0.4
7	...										
8	1.8 ± 0.2										

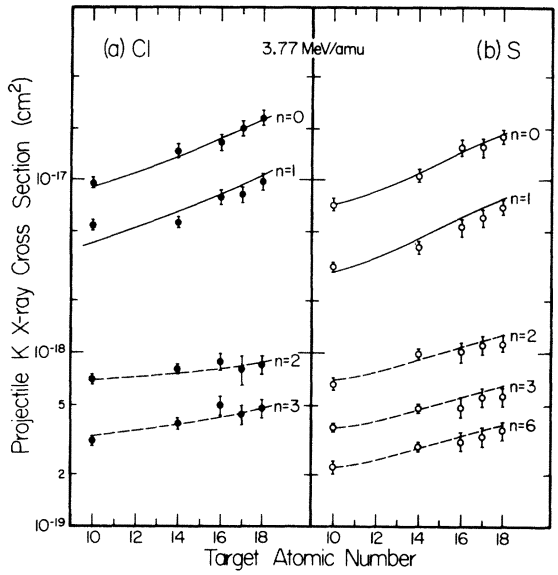

FIG. 7. Projectile K x-ray cross sections as a function of the target atomic number for incident ions carrying n electrons into the collision: (a) for Cl ions (b) for S ions.

different systems. Hence we can represent the projectile x-ray cross section σ^0_{px} by

$$\sigma^0_{px} = fg\sigma^*_{BK}, \tag{1}$$

where σ^*_{BK} is the summation of the Brinkman-Kramers cross section from all shells to all excited states of the projectile. At present, there is no theoretical guidance[18] on how to estimate g. In previous work with fluorine ions, Brown *et al.*[19] have empirically determined this factor in the range $0.06 \leq g \leq 0.10$ by normalizing the results of a BK calculation to measured total electron-capture cross sections. With this normalization a value $f = 0.81$ was obtained for the fraction of capture to excited states that result in x-ray decay. Hopkins *et al.*[7] have normalized x-ray cross section to σ^*_{BK} and have found $fg \simeq 0.07$ for Cl on Kr collisions. For the present set of data with S and Cl bare nuclei, each calculated value of σ^*_{BK} was normalized to σ^0_{px}, and a mean value $\langle fg \rangle = 0.098 \pm 0.0005$ was obtained. In Fig. 8 an excellent fit to the σ^0_{px} data points for the different targets is shown by the broken lines which connect the calculated values of σ^*_{BK} normalized by the single parameter $\langle fg \rangle$. Clearly, the factor-of-3 variation for the electron capture to excited states in these nearly symmetric collisions is accurately reproduced by the calculation. As was shown in Fig. 3, the overall energy dependence of the cross section is reproduced by σ^*_{BK} using the same scaling parameter. The 5% error quoted on the scaling parameter $\langle fg \rangle$ is the standard deviation of the mean of the distribution of the set of fg values and

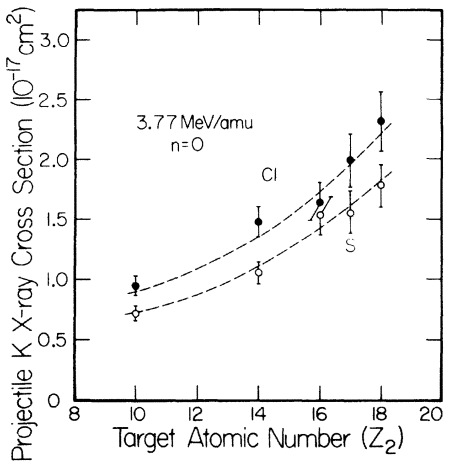

FIG. 8. Projectile K x-ray cross sections for incident bare nuclei at 3.77 MeV/amu as a function of the target atomic number. The broken lines join cross sections for electron capture to all excited states calculated in a Brinkman-Kramers calculation scaled by 0.098.

shows that this single factor gives an accurate scaling of the Brinkman-Kramers cross section for these symmetric collision systems. However, this value is 30% larger than that reported for the more asymmetric collisions of Cl on Kr.[7]

As discussed previously in Sec. III A, it is quite clear that electron capture to excited states determines the cross section for the one-electron incident ions as well as the bare projectiles. Consistent with this conclusion is the similarity in the target dependence for incident states with $n=0$ and 1, apparent in Fig. 7. The experimental cross sections for $n=1$ are smaller than those for $n=0$ by a factor that averages 2.4 ± 0.1 for this set of data. This factor is in close agreement with results reported for fluorine x-ray cross sections,[19] but is considerably smaller than results reported previously for chlorine projectiles.[20] Qualitatively, a factor-of-2 reduction can be estimated by assuming a statistical population of spin states when helium-like P states are formed by electron capture. Then, the six metastable triplet substates ($\Sigma_m {}^3P_{2,0}$) do not decay within the field of view of the detector, while the observed x rays are from the decay of the six short-lived substates ($\Sigma_m {}^{1,3}P_1$). Since this estimate neglects the metastable S states of both hydrogen-like and helium-like ions, as well as the charge dependence of electron capture, nonstatistical populations, and the effects of cascading, it is not definitive but is consistent with the observations of this experiment.

With incident ions carrying two or more electrons into the nearly symmetric collisions with the heavier targets, the projectile cross sections are independent of target atomic number, but for chlorine ions are systematically lower than those for sulphur ions by 18%. In collisions with neon, the cross sections are reduced by 10 to 30% so that the values for both ions are comparable. In all cases, the two-electron ion gives a cross section a factor of 2 larger than the three-electron ion. As discussed previously, this can be attributed to the large cross sections for capture and excitation of a small ${}^3S_1$ metastable component that brings K vacancies into the collisions. For example, if we assume that the metastable state has a cross section for x-ray production comparable to that for $n=1$ ions, then a 5% metastable fraction gives rise to a factor-of-2 increase in the x-ray yield if the ground state has a cross section comparable to that for the $n=3$ ions. Excitation of the metastable ${}^3S_1$ component to the ${}^3P_1$ state would contribute to the observed $K\alpha$ radiation, but not to the $K\beta$ peak. The small, but real, decrease in the observed $K\beta/K\alpha$ intensity ratio for two-electron ions compared to three-electron ions that is evident in Fig. 5 is evidence for metastable excitation.

A further reduction to about 60% of the value for $n=3$ ions occurs in the sulphur cross sections when three additional electrons are present on the incident ion. This reduction is caused by the decreasing fluorescence yield of the K-vacancy state with extra electrons present on the ion. The mean fluorescence yield for these ions[21] is very sensitive to the presence of the last two or three L-shell electrons. Since the $K\alpha$ centroid energies shown in Fig. 4 indicate few L-shell electrons present at the time of emission of $K\alpha$ radiation, the bulk of this radiation arises when L-shell stripping is concurrent with K-vacancy production. However, the state is more likely to Auger decay if the L shell remains intact. The $K\beta$ energy, indicating four L electrons present, suggests that the latter event is more probable. Of course, the Auger decay also competes with the $K\beta$ emission, making the K_β-to-$K\alpha$ ratio continue to fall as seen in Fig. 5 as additional electrons are present on the ion. Because of the difficulty in assessing the fluorescence yield to be used for these ions, any discussion of the processes governing the magnitude of the cross section will be deferred to the discussion of the target cross sections in Sec. III C.

C. Target K x-ray energies and cross sections

The dominance of the projectile radiation (particularly for high charge states), as well as the limited resolution of the detector, make the determination of the spectral distribution of the K x rays from the target atoms rather uncertain in

this experiment. In the data analysis, only single target x-ray groups were identified, and centroid energies and intensities were obtained with the use of the data-stripping procedure[11] that removed a normalized spectrum for the projectile radiation from unresolved spectra. The uncertainty in the centroid energies was ~10 eV for SiK, ~20 eV for S K excited by Cl ions, ~50 eV for Ar K excited by S ions, and greater than this for the other cases. The different targets showed a similar trend in the charge dependence of the centroid energies, and as an example, the results for Si K are shown in Fig. 9. Estimates of the $2p \rightarrow 1s$ transition energy[22] for silicon ions with a single K vacancy but with various numbers of additional L-shell electrons are shown as the horizontal lines on the figure. Spectator electrons in M or higher shells will not change these energies greatly. Significant multiple L-shell ionization of the target occurs along with K-vacancy production in these violent collisions, and in general, one or two more electrons are removed by Cl ions than by S ions. Also, on the average, one or two more electrons are removed by incident bare nuclei of either ion than by the lower charge states.

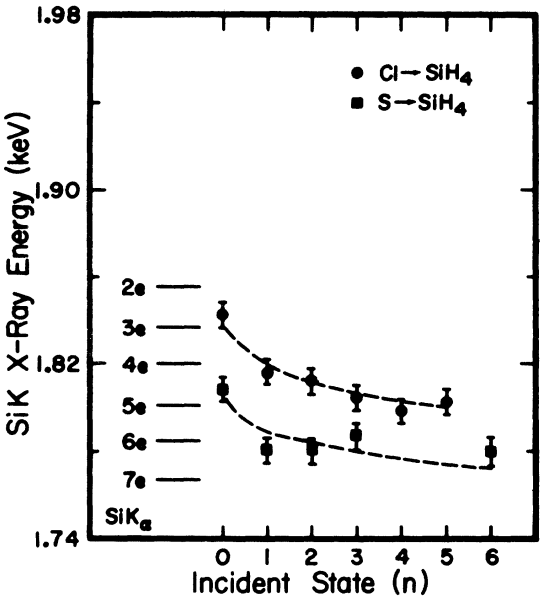

FIG. 9. Observed Si K x-ray energies excited by Cl and S ions carrying n electrons into the collisions. The horizontal lines are theoretical estimates of the Si $K\alpha$ x-ray energy for initial states containing one K-shell vacancy and the indicated number of electrons in the lowest configuration.

Total cross sections for the production of target K x rays by the highly ionized Cl and S projectiles of this experiment are listed in Table II. Trends of the results taken at 3.77-MeV/amu excitation by incident bare nuclei and one- and three-electron ions are illustrated in Fig. 10. Data for the other incident charge states are comparable to that taken with incident three-electron ions and are omitted from the figure for clarity. To guide the eye, broken lines join the points taken with each incident charge state. The absolute uncertainty on each cross section is given in the table and shown by the error bars in the figure. These uncertainties are dominated by the contribution from the spectral analysis.

In the interpretation of these cross sections, the importance of electron capture of target K-shell electrons, predominantly to the projectile K shell, accounts for the large target cross sections observed with incident bare nuclei ($n=0$). However, the mean fluorescence yield that governs the decay of these highly ionized target atoms depends critically on the unknown configuration of the remaining L-shell electrons.

TABLE II. Target K x-ray cross sections (10^{-19} cm^2).

	Chlorine ions					Sulphur ions			
Target / x ray / Incident state $n=Z-q$	105 MeV Si K	132 MeV Si K	132 MeV S K	132 MeV Cl K	132 MeV Ar K	120.7 MeV Si K	120.7 MeV S K	120.7 MeV Cl K	120.7 MeV Ar K
0	14 ± 1.6	13.0 ± 1.6	8.0 ± 1.2	6.3 ± 2	6.6^{+2}_{-3}	8.9 ± 1.1	13 ± 4	14 ± 4	14 ± 2
1	8.1 ± 0.8	6.7 ± 0.6	4.1 ± 0.6	3.3 ± 1	2.4 ± 1	4.8 ± 0.4	4.9 ± 2	5.3 ± 1.5	6.1 ± 0.8
2	4.2 ± 0.4	4.3 ± 0.3	1.9 ± 0.2	1.7 ± 0.6	1.3 ± 0.4	2.9 ± 0.3	2.0 ± 0.6	1.2 ± 0.3	1.8 ± 0.2
3	3.3 ± 0.3	3.3 ± 0.3	1.6 ± 0.2	1.4 ± 0.5	1.6 ± 0.4	2.3 ± 0.2	1.6 ± 0.5	1.3 ± 0.3	1.4 ± 0.2
4	2.9 ± 0.3					...	...	...	...
5	2.5 ± 0.2					...	...	...	...
6	...					1.7 ± 0.2	1.3 ± 0.2	1.2 ± 0.2	1.2 ± 0.2
7	...								
8	1.8 ± 0.2								

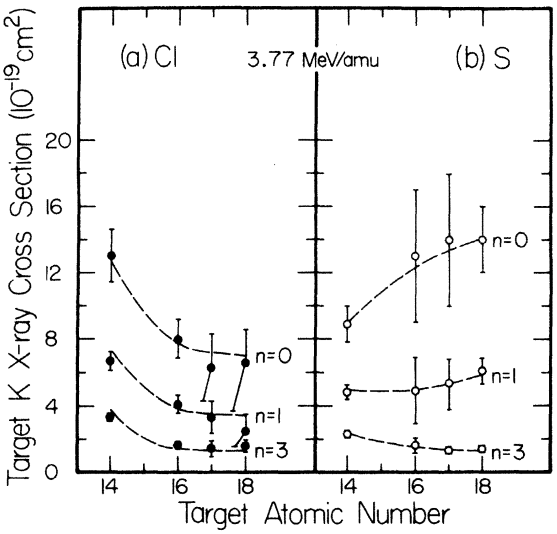

FIG. 10. Target K x-ray cross sections as a function of target atomic number for excitation at 3.77 MeV/amu for incident ions carrying n electrons into the collision. (a) Excitation by Cl ions, (b) by S ions.

In the interpretation of the dependence of the target x-ray cross sections on the projectile charge state, the variation of the mean fluorescence yield $\langle\omega_t\rangle$ of the emitting atoms must be considered. The factor-of-4 increase in cross section that is uniformly observed with the K radiation from all the targets for excitation by bare nuclei over three-electron ions, is unlikely to be caused entirely by variations in $\langle\omega_t\rangle$, for these atoms that have neutral-atom fluorescence yields that vary only a small amount with the removal of the first four L electrons and by a factor of 4 only when the L shell is reduced to two electrons.[21] In fact, similar conclusions[3] for Ar K radiation excited by F ions have been confirmed by measurements of Auger cross sections.[23] The observed $K\alpha$ energies indicate that the difference in degree of ionization for excitation by Cl and S ions is at least as large as the charge-dependent variation. Since the charge dependence in the target x-ray cross sections is similar in the two cases, we conclude that variations in $\langle\omega_t\rangle$ do not dominate the charge dependence, although a gradual variation with charge state may occur, and a value of $\langle\omega_t\rangle$ up to double the neutral atom value may occur even for the low-charge-state ions.

In the interpretation of the mechanisms that produce the cross section variations, both for the target and for the low-charge projectiles, this uncertainty in the fluorescence yield restricts the comparison with theoretical models to general trends. The importance of electron capture of target K-shell electrons accounts for the large target cross sections observed with incident bare nuclei ($n=0$). However, the trend with target atomic number, seen in Fig. 10, for these cross sections is in opposite directions with Cl and S ions. When reasonable estimates of fluoresence yields are considered, the trend with Cl ions cannot be described by the universal scaling of calculated BK capture cross sections, that is successful for all the projectile radiation. For example, if the target K x-ray cross section σ^0_{tx} is assumed to originate entirely from K-shell capture with a calculated cross section σ^K_{BK} [assumed to scale in the same way as the projectile cross section σ^0_{px} in Eq. (1)], then the mean fluorescence yield of the target states can be derived as

$$\langle\omega_t\rangle_D = f\sigma^0_{tx}\sigma^*_{BK}/\sigma^0_{px}\sigma^K_{BK} = f^0_{tx}/\langle fg\rangle\sigma^K_{BK}, \qquad (2)$$

where the factor $f\simeq 0.8$ accounts for capture and cascading that leads to the projectile $2s$ state.[19]

For capture by sulphur nuclei, the derived fluorescence yields are about double the neutral-atom values, qualitatively consistent with expectations for these highly ionized target atoms. Although the same value is derived for Si for capture by Cl, values comparable to neutral-atom fluorescence yields are obtained for S, Cl, and Ar. In fact, the observation of the x-ray energies for the target radiation, as illustrated for Si in Fig. 9, indicates that if any variation exists there should be a higher fluorescence yield for excitation by Cl than for S. We are led to the conclusion that assumptions inherent in Eq. (2) are invalid for these nearly symmetric collisions, even though they have proven valid in previous work with asymmetric collision systems.[1,7,19] The ratio of σ^K_{BK} to σ^*_{BK} ranges from 45% (S on Si) to 18% (Cl on Ar) for these collision systems, but amounts to only a few percent in previous work. This strong variation sensitively tests the assumption in Eq. (2) that the same scaling of the magnitude of Brinkman-Kramers cross sections applies to all target shells for each projectile. The data indicate that this is invalid in these nearly symmetric collisions, and accurate fluorescence yields cannot be obtained with Eq. (2). However, with an accuracy of about a factor of 2, this scaling of σ^K_{BK} accounts for the absolute target cross sections.

Target x-ray cross sections produced by incident one-electron ions are reduced on the average by a factor of 2.2 from the corresponding cross sections produced by bare nuclei. This reduction is comparable to that for the projectile cross sections for these ions. Although the close agreement is surprising, it is somewhat accidental since the projectile data are influenced by the

capture of L electrons to excited states, while the target data is influenced by K-shell transfer. Of course, the mean fluorescence yield for target states excited by one-electron ions may also be lower than for the excitation by bare nuclei.

It is interesting to note that a factor-of-2 reduction in the target cross section with one-electron incident ions is predicted using a molecular model for the K-vacancy sharing[24] by radial coupling between $1s\sigma$ and $2p\sigma$ orbitals. This model has been exploited by Meyerhof[24] to explain vacancy production in a heavier collision partner using initial conditions that have a vacancy in the $2p\sigma$ orbital. If the initial vacancy is in the $1s\sigma$ orbital, however, the model provides an alternative to Born approximation calculations of electron transfer from target K shells by incident projectiles containing K vacancies. The occupation of the $1s\sigma$ orbital corresponds to the K-shell electrons in the highly ionized incident projectiles and the transition probability for the $2p\sigma$ electrons from the target K shell will be large in these symmetric collisions giving a sharing probability $W \simeq \frac{1}{2}$. The target cross section is proportional to the initial $1s\sigma$ occupation number, and hence this model gives a factor-of-2 reduction for incident one-electron ions. The absolute cross section for this mechanism is also proportional to πr_0^2, where r_0 is the effective range at which the radial coupling matrix element is large. Detailed investigations of this aspect of the model have not been carried out, although the observed cross sections can be accounted for by setting r_0 equal to approximately double the target K-shell radius.

For lower-charge-state incident ions, the target cross sections are about 25% of those for incident bare nuclei. Although K-shell capture is reduced for these systems because of the blocked channel in the projectile K shell, it is by no means negligible. For guidance, examination of Fig. 6 shows that about 50% of the cross section calculated in the BK approximation for capture of argon K electrons by chlorine ions is to excited states of the projectile. Somewhat greater fractions are found for the other collision partners. Electron screening will cause a slight reduction in the K capture to excited states for the lower-charge-state ions, but all the observed target radiation can be accounted for by this process.

An alternate description in terms of electron promotion by rotational coupling between filled $2p\sigma$ orbitals and vacant $2p\pi_x$ orbitals can also be used to account for the K-vacancy production by the incident ions with filled K shells.[8] Of course, this process must include vacancy sharing by $2p\sigma$-$1s\sigma$ radial coupling on the outgoing part of the trajectory, as well, so that the total cross section for both target and projectile K vacancies should be included in this discussion. Again, a knowledge of the fluorescence yield for both target and projectile states is necessary to make comparison with the predictions of the model. Through vacancy sharing in these symmetric collisions, the K vacancies are expected to be equally divided between target and projectile; however, the x-ray cross section for the former is only about $\frac{1}{3}$ of the latter. Since the incident three-electron projectiles for both S and Cl are expected to have a fluorescence yield of about 0.6 (if the two L-shell electrons remain on the ion but are distributed in the L shell by $2s$-$2p$ excitation[25]), a value of 0.2 for the target states excited by these ions is assumed. With these gross simplifications, the total K-vacancy cross sections estimated from the measured x-ray cross sections with incident three-electron ions have been obtained and are listed in Table III.

Also shown in Table III are the $2p\sigma$-$2p\pi_x$ rotational coupling cross sections calculated using the universal scaling for this process recently published by Taulbjerg *et al.*[8] The close agreement between the experimental and theoretical cross sections is somewhat fortuitous, considering the assumptions used in estimating the fluorescence yields. However, that the molecular model correctly describes these cross sections at a scaled velocity near unity gives us evidence that the simple universal scaling of the $2p\pi$-$2p\sigma$ cross section is valid over a wide velocity range.

IV. CONCLUSION

K x-ray energies and cross sections have been measured, under single-collision conditions for charge transfer, as a function of the incident charge state of highly ionized S and Cl ions. For incident bare nuclei, the dependence of the projectile cross sections on the target atomic number are accurately reproduced for both ions by scaling cross sections for capture to excited states calculated in a Brinkman-Kramers approximation by a single normalization constant. The magnitude

TABLE III. Total K-vacancy cross sections σ_v(expt.) for three-electron incident ions at 3.77 MeV/amu. Mean fluorescence yields of 0.6 and 0.2 were assumed for projectile and target radiation, respectively. Cross sections σ_v(calc.) were calculated using the rotational coupling of $2p\pi_x$-$2p\sigma$ orbitals. All units are 10^{-19} cm^2.

Projectile	Cl				S			
Target	Si	S	Cl	Ar	Si	S	Cl	Ar
σ_v(expt.)	23	16	14	16	18	16	16	16
σ_v(calc.)	24	20	18	17	26	22	20	18

of the target cross section is also reproduced by the same scaling of calculated cross sections for capture of K-shell electrons. However, the details of the cross section for different targets is inconsistent with the trends of the calculated results.

With one-electron ions incident, the cross sections are reduced by factors of 2.4 and 2.2 for the projectile and target, respectively. The reason for this reduction is different in the two cases, being qualitatively explained by lifetime arguments in the former case, but by the $1s\sigma$ occupation number in the latter.

For the lower-charge-state ions, the mean fluorescence yield of the emitting states is estimated using vacancy-sharing arguments. Total K-vacancy production cross sections are found to be in excellent agreement with the values calculated using rotational coupling of $2p\pi$-$2p\sigma$ orbitals, even at a scaled velocity near unity.

V. ACKNOWLEDGMENTS

We thank the most able and cooperative BNL Tandem Accelerator staff for their help in conducting this experiment. One of us (J.R.M.) acknowledges computational assistance of J. A. Guffey and C. P. Bhalla, and useful discussions with C. L. Cocke, during the data analysis and preparation of this paper.

---

*Research supported in part by U. S. Energy Research and Development Administration Contract E(11-1)-2753 and ONR; the experiment was carried out at the BNL Tandem Accelerator Laboratory.

†Present address: Naval Surface Weapons Ctr-223, White Oak, Silver Springs, 20910.

‡Present address: LASL-Laser Group L1, P. O. Box 1663, Los Alamos, N. M. 87544.

§Present address: Dept. of Physics, East Carolina University, Greenville, N. C. 27834.

||Present address: Dept. of Physics, New York University, New York, N. Y. 10003.

¶Present address: Dept. of Physics, City College CUNY, New York, N. Y. 10031.

[1]J. R. Macdonald, L. M. Winters, M. D. Brown, T. Chiao, and L. D. Ellsworth, Phys. Rev. Lett. 29, 1291 (1972); J. R. Mowat, D. J. Pegg, R. S. Peterson, P. M. Griffin, and I. A. Sellin, Phys. Rev. Lett. 29, 1577 (1972); F. Hopkins, R. Brenn, A. R. Whittemore, N. Cue, V. Dutkiewicz, and R. P. Chaturvedi, Phys. Rev. A 13, 74 (1976).

[2]D. Burch, N. Stolterfoht, D. Schneider, E. Wieman, and J. S. Risley, Phys. Rev. Lett. 32, 1151 (1974).

[3]L. M. Winters, J. R. Macdonald, M. D. Brown, T. Chiao, L. D. Ellsworth, and E. W. Pettus, Phys. Rev. A 8, 1835 (1973); C. W. Woods, R. L. Kauffman, K. A. Jamison, C. L. Cocke, and P. Richard, J. Phys. B 7, L474 (1974).

[4]R. L. Kauffman, C. W. Woods, K. A. Jamison, and P. Richard, Phys. Lett. 50A, 75 (1974).

[5]A. M. Halpern and J. Law, Phys. Rev. Lett. 31, 4 (1973).

[6]B. Fastrup, E. Bøving, G. A. Larsen, and P. Dahl, J. Phys. B 7, L206 (1974); N. Stolterfoht, D. Schneider, D. Burch, B. Aagaard, E. Bøving, and B. Fastrup, Phys. Rev. A 12, 1313 (1975).

[7]F. Hopkins, N. Cue, and V. Dutkiewicz, Phys. Rev. A 12, 1710 (1975).

[8]K. Taulbjerg, J. S. Briggs, and J. Vaaben, J. Phys. B 9, 1351 (1976).

[9]L. M. Winters, M. D. Brown, L. D. Ellsworth, T. Chiao, E. W. Pettus, and J. R. Macdonald, Phys. Rev. A 11, 174 (1975).

[10]All the spectra were printed digitally, plotted graphically, and stored on magnetic tape at BNL. At KSU, the data were analytically fit using the graphical output for guidance, and normalized absolutely to the number of counts in the digital output after subtracting the number of counts in the background spectra.

[11]The composite spectrum for each projectile charge state was normalized by peak height prior to subtraction from the spectrum to be stripped.

[12]The detector window is removable and the transmission function has been measured. The results are consistent with the absorption curve calculated for this window and shown in L. M. Winters, J. R. Macdonald, M. D. Brown, L. D. Ellsworth, and T. Chiao, Phys. Rev. A 7, 1276 (1973).

[13]Charge-exchange cross sections have not been reported for these highly ionized ions, but were estimated from the measured projectile x-ray cross sections of this experiment.

[14]J. R. Macdonald, E. Salzborn, L. D. Ellsworth, and J. A. Guffey (unpublished); E. Salzborn, J. A. Guffey, L. D. Ellsworth, and J. R. Macdonald, Bull. Am. Phys. Soc. 20, 639 (1975).

[15]The calculation uses hydrogen-like wave functions for closed target shells and give total cross sections from a particular target shell to all angular momentum states of a given principal quantum number in the projectile. The closed form expression for the cross section is given by V. S. Nikolaev, Zh. Eksp. Teor. Fiz. 51, 1263 (1966) [Sov. Phys.-JETP 24, 847 (1967)].

[16]C. L. Cocke, B. Curnutte, J. R. Macdonald, and R. Randall, Phys. Rev. A 9, 57 (1974); C. L. Cocke, B. Curnutte, and R. Randall, Phys. Rev. A 9, 1823 (1974). The energies shown are the mean energy of the multiplets formed with each charge state.

[17]C. P. Bhalla (private communication).

[18]For example, see the conclusions drawn by A. M. Halpern and J. Law, Phys. Rev. A 12, 1776 (1975).

[19]M. D. Brown, L. D. Ellsworth, J. A. Guffey, T. Chiao, E. W. Pettus, L. M. Winters, and J. R. Macdonald, Phys. Rev. A 10, 1255 (1974).

[20]J. R. Mowat, I. A. Sellin, P. M. Griffin, D. J. Pegg, and R. S. Peterson, Phys. Rev. A 9, 644 (1974).

[21]C. P. Bhalla, Phys. Rev. A 8, 2877 (1973).

[22]L. L. House, Astrophys. J. Suppl. Ser. 18, 21 (1969).

[23]C. L. Cocke, R. R. Randall, and B. Curnutte, in *Abstracts of the Papers on the Ninth International Conference on the Physics of Electronic and Atomic Collisions*, edited by J. S. Risley and R. Geballe (Univ. of Washington Press, Seattle, 1975), Vol. 2, p. 933.

[24]J. S. Briggs and K. Taulbjerg, J. Phys. B 8, 1919 (1975); W. E. Meyerhof, Phys. Rev. Lett. 31, 1341 (1973).

[25]J. R. Macdonald and E. H. Pedersen, Bull. Am. Phys. Soc. 20, 674 (1975).